ACS OMEGA

http://pubs.acs.org/journal/acsodf

Article

Effects of S and Al on K Migration and Transformation during Coal and Biomass Co-combustion

Qian Liu,* Wenqi Zhong, Jun Zhou, and Zuowei Yu

Cite This: *ACS Omega* 2022, 7, 15880−15891

Read Online

ACCESS | Metrics & More | Article Recommendations

ABSTRACT: The co-combustion of biomass and coal has both environmental and economic benefits in terms of pollutants and greenhouse gas emissions. However, one of the key factors affecting the feasibility of this technology is the ash deposition and corrosion caused by the high alkali metal content of biomass, especially K. After the addition of elemental S to corn stalk/Xiaolongtan lignite blended fuel and Al_2O_3 to corn stalk/Datong lignite, combustion experiments were carried out in a tubular furnace to explore the effects of S and Al in coal on K migration and transformation. The experimental results show that when S/K < 6, an increase in the S/K ratio inhibited the release of K. When S/K > 6, the sulfation become saturated, and an increase in S promoted the release of K. When S/K = 6, the higher the temperature was, and the more obvious the inhibitory effect on the release of K was. Increasing the S/K ratio not only increased the $CaSO_4$ content of the ash but also increased the content of water-soluble K compounds, such as K_2SO_4, and decreased the contents of acid-soluble K compounds and insoluble K compounds, such as $KAlSi_3O_8$. After Al_2O_3 was added, as the Al/K ratio increased, the K release rate gradually decreased. When the sample with Al/K = 2.5 and the original samples were burned at 600−700 °C, the difference in the K release rates of the two samples was relatively small. When the temperature was higher than 700 °C, the higher the temperature was, and the greater the difference in the K release rates of the samples was, which indicates that a high temperature promotes the formation of aluminosilicates containing K.

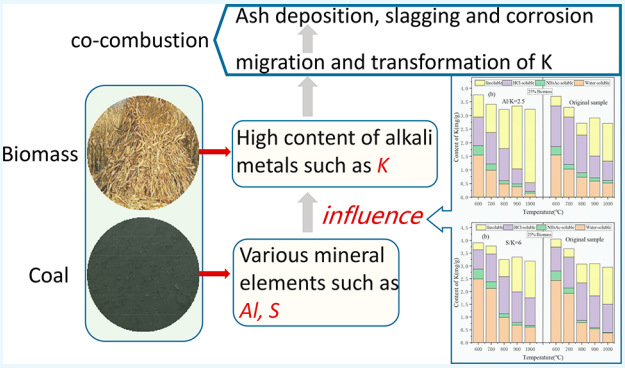

1. INTRODUCTION

The co-combustion of biomass and coal has both environmental and economic benefits in terms of pollutants and greenhouse gas emissions.[1] Not only can it reduce the combustion of traditional fossil fuels and save energy, but it also effectively improves the combustion performance of the fuel compared with pure biomass combustion, which is conducive to improving boiler efficiency.[2] Moreover, the cost of converting existing coal-fired power plants into biomass-coal cofired power plants is lower than the cost of establishing new biomass power plants.[3] In addition, in order to minimize the fluctuating supply of some secondary fuels and ensure the safety of power generation, a flexible method (i.e., different proportions of secondary fuels) can be adopted for co-combustion, which is certain to produce huge economic benefits.[4] Compared with coal combustion, the mixed combustion of coal and biomass can significantly reduce the release of pollutants such as SO_x and NO_x, which makes this a clean combustion technology with low carbon emissions.[5]

However, one of the key factors affecting the feasibility of this technology is the ash deposition and corrosion caused by the high alkali metal content of biomass.[6] Because of the relatively high K content of biomass (especially herbs), during the process of mixed combustion, alkaline substances (e.g., KCl) may be transformed to the gas phase due to their high chemical activity, resulting in ash accumulation, slagging, and corrosion on the boiler heating surface, which leads to a reduced heat transfer capacity, increased heat loss, deviation from the designed operation of the boiler, and a greatly reduced boiler operation efficiency.[7−9] During the co-combustion process, the alkali metals in the biomass will react with the inorganic minerals in the coal to produce low-temperature melts and volatile alkali metal compounds, making the ash composition more complicated.[10−12] Therefore, it is particularly important to study the migration, transformation, and deposition behaviors of alkali metals during the process of biomass-coal combustion to ensure the safe and efficient operation of the boiler.

Regarding the occurrence forms of alkali metals, the current research method mainly involves chemical step-by-step

Received: February 18, 2022
Accepted: April 20, 2022
Published: April 29, 2022

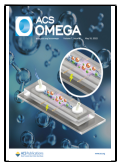

extraction of samples, sampling, and classification of samples at different stages.[10−13] This method has a wide range of applications in experimental research and industry. Generally, the solid-phase occurrence of alkali metals can be divided into four categories via extraction separation.[14−16] (1) Water-soluble alkali metals: alkali metals that are soluble in water, such as KCl, K_2SO_4, and K_2CO_3. (2) Ammonium acetate soluble alkali metals: alkali metals bonded with oxygen-containing functional groups such as a carboxyl group, which can be plasma exchanged with NH_4^+. (3) Hydrochloric acid soluble alkali metals: including other forms of alkali metals in addition to aluminosilicates and those wrapped by a carbon matrix, such as silicates containing alkali metals. (4) Insoluble alkali metals: alkali metals that are insoluble in hydrochloric acid, sulfuric acid, and other general acids but are soluble in hydrofluoric acid, mainly including aluminosilicates containing alkali metals.

Because the fuel characteristics of coal and biomass are very different, and their ash compositions are not the same, the alkali metals and alkaline earth metals in biomass fuel easily combine with the inorganic minerals in coal during their co-combustion, resulting in volatile alkali metals and a low-temperature eutectic, which seriously affects the safe and efficient operation of the currently available thermal equipment.

Wei et al.[17] analyzed the influence of other elements on alkali metal release during the co-combustion of straw and coal, and they found that Si, Al, Ca, Mg, and S can greatly affect the behavior of Cl, K, and Na, while other minor elements (e.g., Fe, Ti, and Mn) have little influence. During co-combustion, most of the potassium is released as $KCl_{(g)}$, $KOH_{(g)}$, and $K_2SO_{4(g)}$ since aluminum preferentially combines with Ca and Mg to form corresponding compounds, such as $Ca_3Al_2O_6$, $CaAl_2O_4$, and $MgAl_2O_4$. When there are more aluminum and silicon in the mixed fuel, most of the potassium exists as solid $KAlSi_2O_6$, and less than 10% of the potassium precipitates in the form of gaseous $KC1_{(g)}$ and $KOH_{(g)}$. Gaseous $KC1_{(g)}$, $KOH_{(g)}$, $K_2SO_{4(g)}$, and molten $K_2Si_4O_9$ are easily deposited on the heat exchange surface, resulting in serious ash deposition. Glazer et al.[18] studied the migration and transformation of alkali metals during the co-combustion of coal and biomass in a circulating fluidized bed, and they found that the ash forming elements in coal and biomass have a great impact on the release of alkali metals. The release of alkali metals is mainly affected by the Cl content rather than the contents of the alkali metals. In addition, the silicon and aluminum in the fuel will inhibit the release of alkali metals, but it will form alkali metal silicates with low melting points, resulting in ash deposition and agglomeration problems. The use of biomass and coal with complementary compositions significantly reduces the release of alkali metals.

Yang et al.[19] studied the effect of the sulfur in coal on the behaviors of alkali metal during the co-combustion of biomass and coal. Their results revealed that when the S/K molar ratio was >2, the production of potassium sulfate increased greatly with the addition of FeS_2. In addition, increasing the dosage of FeS_2 can reduce the formation of $KCl_{(g)}$ and $KOH_{(g)}$ and promote the release of $HCl_{(g)}$. Johansen et al.[20] studied the release of potassium, chlorine, and sulfur during the combustion of high chlorine biomass in small and pilot-scale test benches and found that the release of K increased during combustion in larger fuel beds, while the release of Cl significantly decreased in the temperature range of 900−1000 °C. As the proportion of low chlorine sawdust increased, the form of Cl changed from a high concentration of HCl to KCl. Li et al.[21] studied the influence of temperature on the release and transformation of alkali metals during the co-combustion of coal and sulfur-rich wheat straw. Their results revealed that the presence of Fe, Ti, S, Si, and Al in the mixture can reduce the release of K and Na during co-combustion. Theis et al.[22] found that when peat/bark and peat/straw mixtures were burned, the deposition rate began to increase only when the Cl/S molar ratio of the feed ash exceeded 0.15. During the co-combustion of peat and bark, sulfur can sulfate alkali metals, reduce the content of KCl in ash, and inhibit ash deposition. Wang et al.[23] found that high contents of potassium silicate and phosphate in the ash led to serious coking problems, and adding Ca to reduce the K/Ca ratio promoted the production of calcium silicate and calcium phosphate and reduced the coking problems.

The above-mentioned research indicates that the inorganic elements in coal have an important influence on the release of K and the ash deposition and slagging caused by the release of K during co-combustion. However, quantitative analysis of the influences of the inorganic elements in coal on the release of K, the transformations between the occurrence forms of K, and the influence of the crystalline phase of the ash is still lacking. These analyses are of great significance to reducing the ash deposition and slagging caused by alkali metals during co-combustion, to further increasing the biomass blending ratio, and to further development of biomass-coal co-combustion technology.

Compared with biomass, the Al and S contents of coal are much higher, and these elements affect the migration and transformation of K. Coal has a much higher sulfur content than biomass. In the co-combustion of biomass and coal, the volatile alkali metals in the biomass are retained in the solid phase through reactions with the sulfur in the coal in the form of alkali metal sulfates, thus reducing the content of alkali metal chlorides in the sediments with low melting points, alleviating the problems caused by slagging, corrosion, and bed material agglomeration, and reducing the release of SO_2. The reduction of both alkali metal mitigation and acid gas emissions can be achieved in an economical and environmentally friendly manner.

The sulfur in coal exists in three forms: inorganic sulfur, organic sulfur, and elemental sulfur.[24] Elemental sulfur is one of the most important forms of sulfur in coal. Furthermore, pyrite is the most abundant sulfur mineral in coal, but several other sulfide minerals can be present. During coal combustion, first, the pyrite is decomposed into elemental sulfur and ferrous sulfide, and then, the S can react with H and CO to produce H_2S and COS, or it can be directly polymerized to S_n.[25] Therefore, elemental S and Al_2O_3 were added to the raw materials in this study to explore the effects of S and Al in coal on the migration and transformation of K during co-combustion in order to determine the optimum S/K and Al/K ratios for actual combustion.

2. MATERIALS AND METHODS

2.1. Materials. Corn stalks (CS) from Donghai, Jiangsu Province, were chosen as a representative form of biomass. Lignite from Xiaolongtan, Yunnan Province (XL), and lignite from Datong, Shanxi Province (DL), were selected as representative coal samples. All of the materials were crushed and sieved, and the <0.18 mm fraction was selected for the

https://doi.org/10.1021/acsomega.2c00994
ACS Omega 2022, 7, 15880−15891

Table 1. Results of Proximate and Ultimate Analyses of Samples (wt %, ad)

	ultimate analysis				proximate analysis				
samples	C	H	O	N	S	M	ash	VM	FC
CS	42.13	6.29	36.72	1.27	0.15	4.26	9.17	72.57	14.00
XL	46.56	3.72	17.90	1.38	1.46	13.90	15.08	39.53	31.49
DL	60.87	4.57	7.79	1.10	2.71	5.94	17.03	31.09	45.94

Table 2. Ash Compositions of the Samples

samples	K_2O	Na_2O	MgO	CaO	Fe_2O_3	SiO_2	Al_2O_3	P_2O_5
CS	31.01	0.41	1.46	4.02	0.35	31.48	5.34	8.35
XL	0.96	0.27	2.34	39.16	9.58	21.13	13.32	0.07
DL	0.05	0.23	1.86	9.70	27.71	28.72	12.57	0.08

Table 3. Al and K Contents in the Raw Materials

samples	Al (wt %)	total K (mg/kg)	water-soluble K (wt %)	NH_4Ac-soluble K (wt %)	HCl-soluble K (wt %)	insoluble K (wt %)
CS	0.001	16531.22	84.61	5.22	3.21	6.96
XL	0.171	370.26	5.27	21.73	67.84	5.16
DL	0.165	41.31	8.41	35.16	30.46	25.97

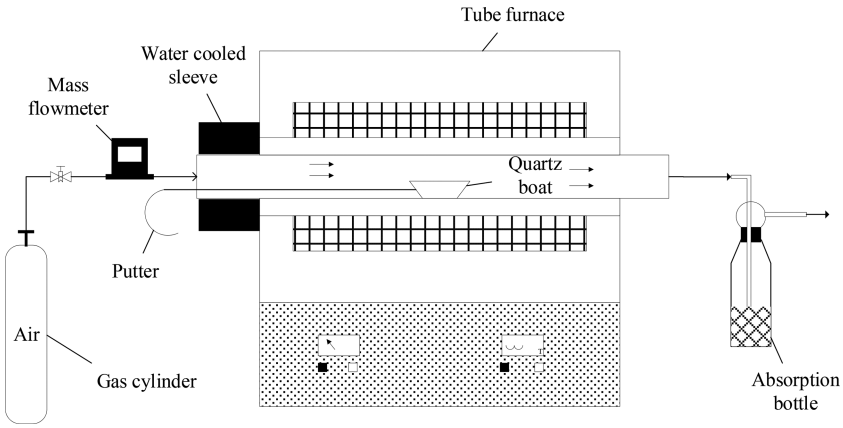

Figure 1. Schematic diagram of the combustion device used in the experiments.

experimental study. The proximate analysis of the samples was carried out according to standards ASTM D 3173-03 (M), ASTM D 3174-04 (Ash), ASTM D 3175-07 (VM), and the FC (fixed carbon) value was determined by subtracting the sum of M (moisture), Ash, and VM (volatile matter) from 100%. The ultimate analysis of the samples was conducted using an Elementar Unicube elemental analyzer. The results of the proximate analysis and ultimate analysis of the materials are presented in Table 1. An X-ray fluorescence spectrometer (XRF, Shimadzu XRF1800, Japan) was used to analyze the ash content of the materials, and the results are presented in Table 2. As can be seen from Table 1, the volatile content of the biomass was much higher than that of the coal, while the S content of the coal was much higher than that of the biomass, and the S content of DL was the highest. Table 2 shows that the K content of the corn stalk ash was higher, the Ca content of the XL ash was the highest, the Fe content of the DL ash was higher, and the Al content of XL was slightly higher than that of DL. Since the maximum biomass blending mass ratio in most power plants is about 20−30%,[26] the biomass blending ratio in this experimental study was set as 25%.

2.2. Analytical Methods. The chemical step-by-step extraction method is widely used to measure the contents of alkali metals (K, Na), and the specific method used in this study was as follows.[27] A 200 mg sample (raw material or ash sample) was dissolved in 50 mL of deionized water at 60 °C and stirred for 24 h. After filtration, the content of the water-soluble K in the filtrate was measured via inductively coupled plasma-optical emission spectrometry (ICP-OES, iCap-6300, America). Then, the filtrate was successively dissolved in 1 M NH_4Ac solution and 1 M HCl solution. The above steps were repeated to obtain the NH_4Ac-soluble K content and HCl-soluble K content, respectively. Finally, the filter residue was digested using a microwave digestion instrument (Mars, America), and the insoluble K content was determined via ICP-OES. The Al content of the raw material was directly digested in the digester and was measured via ICP-OES. The K and Al contents of the raw materials are presented in Table 3. The Al content of the coal was much higher than that of the biomass, and the Al content of XL was the highest. The K content of the biomass was much higher than that of the coal, and it mainly existed in the form of water-soluble K. The crystalline phases in the samples were measured using an X-ray diffractometer (XRD, Bruker D8 Advance, Germany), with a Cu K-α target, a scanning speed of 4°/min, and a scanning range of 5−90°.

2.3. Experimental Apparatus and Methods. The combustion experiment was carried out in an electric heating

https://doi.org/10.1021/acsomega.2c00994
ACS Omega 2022, 7, 15880−15891

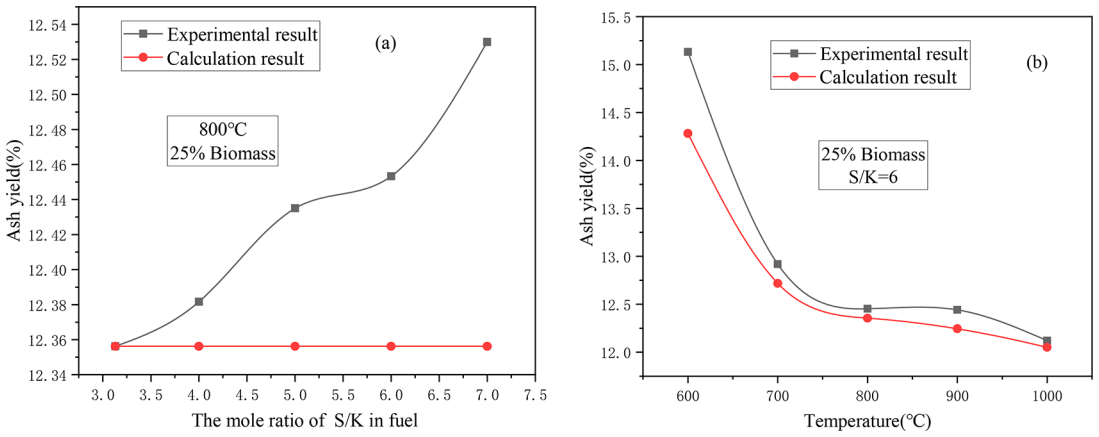

Figure 2. Effects of adding S on the ash yield of CS/XL: (a) ash yield under different S/K mole ratios; and (b) ash yield at different temperatures.

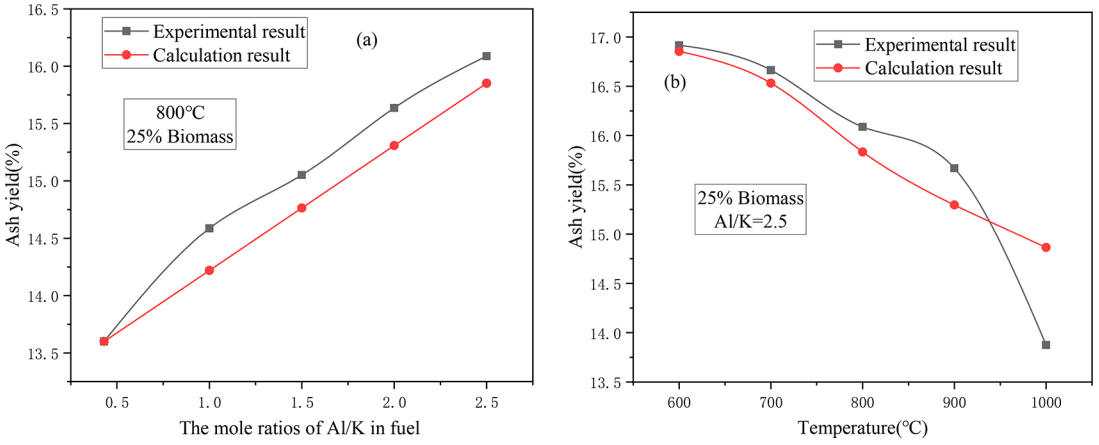

Figure 3. Effect of adding Al_2O_3 on the ash yield of CS/DL: (a) ash yield under different Al/K molar ratios; and (b) ash yield at different temperatures.

tube furnace (Figure 1), with a maximum heating temperature of 1050 °C. The tube was composed of quartz, with an inner diameter of 54 mm and a length of 1 m. There was a cold-water sleeve at the left end of the tube furnace to cool the sample. Air was supplied through high-pressure steel cylinders. In each run, 4 g of fuel was evenly spread in a quartz boat and was placed in the cooling section at the left end of the instrument. The air flow rate was 1 L/min. The tube furnace was heated to the specified temperature, and then, the quartz boat was pushed into the heating section of the furnace using a push rod, and the exhaust gas was connected to the flue gas analyzer to determine whether the reaction was over. The reaction time was controlled at 70 min, at which time the reaction was over under all of the operating conditions. Finally, the ash samples were removed from the furnace and analyzed.

Because the S content of XL was lower, the Al content of DL was lower, and the biomass blending ratio was 25%, the S/K molar ratio of the CS/XL raw material was 3.13, and the Al/K molar ratio of the CS/DL raw material was 0.43. Therefore, elemental S was added to the CS/XL to achieve S/K molar ratios of 4, 5, 6, and 7. The effects of the different S/K molar ratios on the K migration and transformation were investigated, and the combustion temperature was changed while S/K = 6 was maintained to explore the effects of S on the migration and transformation of K at different temperatures. Al_2O_3 was added to the CS/DL material to make mixtures with Al/K molar ratios of 1, 1.5, 2, and 2.5 in order to explore the effect of the Al/K molar ratio on the K migration and transformation. The combustion temperature was changed while maintaining Al/K = 2.5 to explore the effect of Al on the migration and transformation of K at different temperatures.

3. RESULTS AND DISCUSSION

3.1. Influences of S and Al in Coal on the Ash Yield.

After the combustion of the raw materials, the mass of the ash sample was weighed, and the ash rate was calculated using eq 1.

$$A = \frac{m_{ash}}{m_{fuel}} \times 100\% \quad (1)$$

where A is the ash yield, m_{fuel} is the mass of the raw material, and m_{ash} is the mass of the ash sample after combustion. The ash yield can initially reflect the release of the inorganic substances in the ash, and it can be used to calculate the K release rate. In addition, the theoretical ash yield was calculated based on the assumption that there was no interaction between the coal and biomass during the combustion and that the S was converted into SO_2 and released.

The ash yield of CS/XL after adding S is shown in Figure 2. The original S/K of the raw material was 3.13. After the addition of S, theoretically S should be converted into SO_2 and released, and the ash yield should not change as the S/K ratio increases. However, it was found that in the experiments, as the S increased, the ash yield gradually increased, indicating that

https://doi.org/10.1021/acsomega.2c00994
ACS Omega 2022, 7, 15880−15891

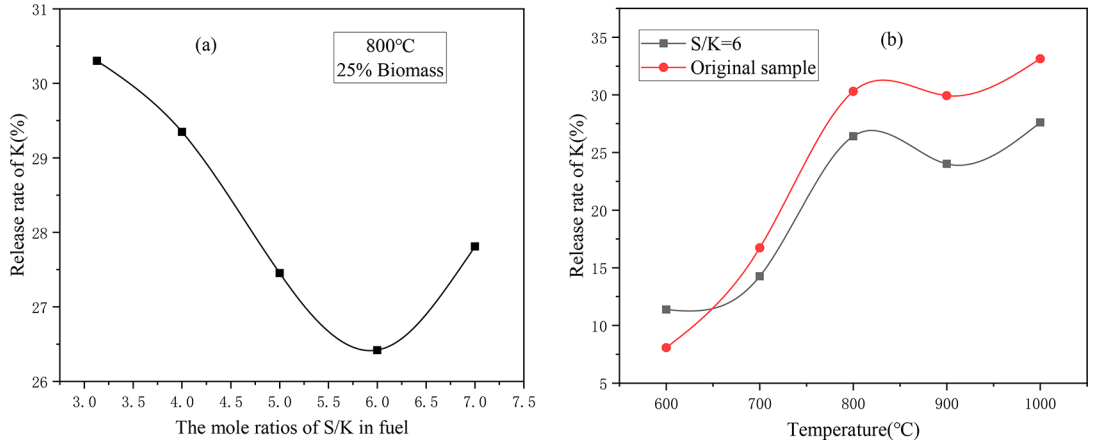

Figure 4. Effect of adding S on the K release rate of CS/XL: (a) K release rates for different S/K mole ratios; and (b) K release rates at different temperatures.

the added S was not completely released, and it reacted with the raw materials and was fixed in the ash. The actual ash yield increased at a variable rate as the S/K ratio increased. When the S/K ratio was 3.13−5 and 6−7, the ash yield increased rapidly with the addition of S, but when the S/K ratio was 5−6, the ash yield did not change significantly. This indicates that different reactions will occur under different S/K ratios, resulting in different amounts of S being fixed in the ash.

Figure 2b shows the curve of the ash yield versus temperature for a sample with S/K = 6. It can be seen that as the temperature increased, both the actual ash yield and the theoretical ash yield gradually decreased, and the trends of both were very similar to that of the change in temperature. However, there were some differences between the actual ash yield and the theoretical ash yield in the different temperature ranges. When the temperature was between 600 and 800 °C, the actual ash yield was always higher than the theoretical ash yield, and the difference between them decreased gradually with increasing temperature. This is mainly because the increase in temperature promoted the release of SO_2. However, when the temperature was between 800 and 1000 °C, the difference between the actual yield and the theoretical ash yield initially increased and then decreased with increasing temperature, which may have been caused by the melting of ash samples when the temperature was higher than 800 °C. The melting of the ash samples increased the resistance to the diffusion of SO_2 from inside the fuel to the surface and inhibited the release of SO_2.

Figure 3 shows the ash yield of CS/DL after adding Al_2O_3. Figure 3a shows the ash yield curves for different Al/K molar ratios. For the theoretical ash yield, the reaction between Al_2O_3 and the fuel is not considered after the Al_2O_3 is added. After the addition of Al_2O_3, the actual ash yield was always higher than the theoretical ash yield. It was found that for the various Al/K ratios, the actual ash yield was always higher than the theoretical ash yield, but the difference was not large, and it is much smaller than the difference between the theoretical and actual ash yields after adding S. This indicates that Al_2O_3 may be less reactive and less effective in fixing the gas phase substances.

Figure 3b shows the variation of the ash yield with temperature for Al/K = 2.5. In the different temperature ranges, the variations in theoretical and actual ash yields were also not the same. At 600−800 °C, the actual ash yield was higher than the theoretical ash yield, but the difference between the two was not large, indicating that within this temperature range, Al_2O_3 had a certain fixation effect on the release of the gas phase substances. When the temperature was about 800−900 °C, the difference between the actual and theoretical ash yields increased, indicating that within this temperature range, the reaction activity of Al_2O_3 was stronger, and more gas-phase substances were fixed in the ash. When the temperature was higher than 900 °C, the difference between the theoretical and the actual ash yields gradually decreased. In particular, when the combustion temperature was 1000 °C, the actual ash yield was much lower than the theoretical ash yield. It is preliminarily speculated that a high temperature may promote the reaction of the Ca in ash with Si and Al to form aluminosilicates, which results in less Ca binding to S and promotes the release of SO_2.

3.2. Influence of S and Al in Coal on the Release and Transformation of K during Co-Combustion. Combined with the ash yield, the release rate of K under various operating conditions was calculated using eq 2:

$$R = \left(1 - \frac{A \times C_{ash}}{C_{fuel}}\right) \times 100\% \quad (2)$$

where R is the release rate of K, and A is the ash yield. C_{ash} is the total concentration of K in the ash sample, and C_{fuel} is the total concentration of K in the raw material. The release rate of K can reflect the proportion of the K in the raw material that is released into the gas phase.

In addition, after combustion, the ash samples were chemically extracted step-by-step to investigate the conversions between the different occurrence forms of the K. For the convenience of comparison, the results of the alkali metal occurrences were converted into the alkali metal contents retained in the initial 1 g of fuel using eq 3:

$$M = N_{ash} \times A \quad (3)$$

where M is the K concentration of the different occurrence forms in the raw material, N_{ash} is the concentration of the different occurrence forms of K in the ash, and A is the ash yield.

The K release rate of CS/XL under different S/K molar ratios after adding S is shown in Figure 4. When S/K < 6, the release rate of K gradually decreased with increasing addition of S, indicating that the addition of S cause more K to be fixed

https://doi.org/10.1021/acsomega.2c00994
ACS Omega 2022, 7, 15880−15891

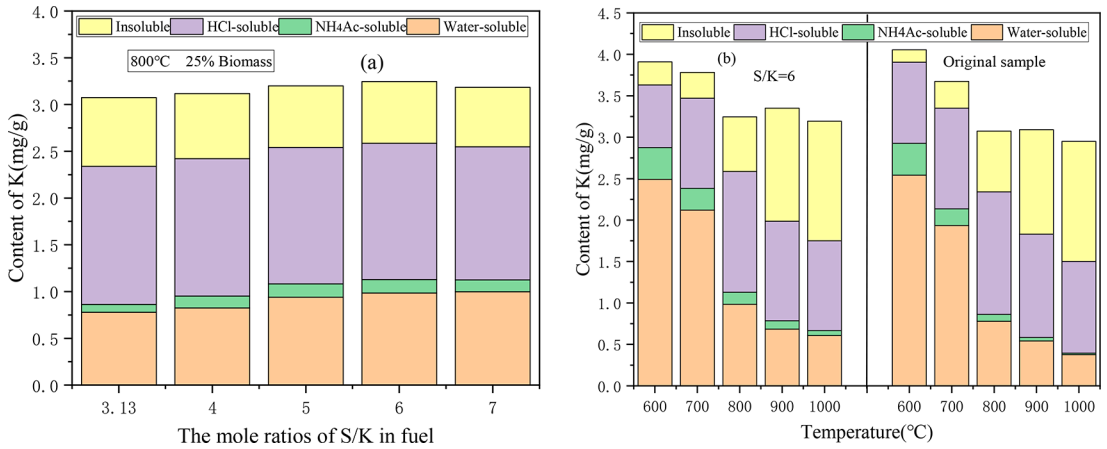

Figure 5. Effect of adding S on the retention of the different occurrence forms of K in the CS/XL ash: (a) the occurrence forms of K under different S/K mole ratios; and (b) the occurrence forms of K at different temperatures.

in the ash sample. The main reason for this phenomenon may be that the addition of S promotes Reaction (R1),[7,28] and thus, a large amount of KCl is converted into K_2SO_4, reducing the release rate of K. When S/K > 6, the release rate of K increased with increasing addition of S. The release rate of K initially decreased and then increased as the S/K ratio increased, which has also been reported in previous studies. The possible reason for this is that when the S/K ratio increased to six, the sulfation of the KCl became saturated.[19] In addition, when the K_2SO_4 content was sufficiently high, KCl and K_2SO_4 were still below the eutectic at low temperatures, making the melting point of the eutectic compound lower than that of KCl, thus promoting the release of water-soluble K.[29]

$$4KCl + 2SO_2(g) + O_2(g) + 2H_2O(g) \rightarrow 2K_2SO_4 + 4HCl(g) \quad (R1)$$

Figure 4b shows the K release rates of the sample with S/K = 6 and the original sample at different temperatures. The trend of the K release rate with temperature is similar before and after the addition of S, and the K release rate decreased as the temperature increased from 800 to 900 °C. Generally, the release of K is a process in which gaseous potassium compounds move from the interior of the ash particles to the surfaces of the ash particles, resulting in a higher release of K from finer fuel particles than from coarser fuel particles. In addition, the higher the temperature is, the more easily the gaseous potassium compounds can migrate from the interior to the surface, thus increasing the release rate.[30,31] From the physical and chemical properties of the ash, it is known that the ash samples melt at high temperatures. This can enhance the fixation reaction between the potassium and silicon aluminum minerals. In addition, it can also increase the resistance of the release of the K in the sample into the gas phase, thus reducing the ability to release K in this temperature range.[32] When the temperature was between 900 and 1000 °C, the release rate of K began to increase again with increasing temperature, which indicates that the release of K was affected by two factors. The increase in temperature increased the power of the gaseous potassium compounds to move from the inside to the surface of the ash sample, but the increase in temperature caused the ash sample to melt, which increased the resistance to the internal potassium being released to the gas phase. When the temperature was higher than 900 °C, the effect of the temperature on the release of K was stronger. When the temperature was between 650 and 1000 °C, the K release rate after the addition of S was always lower than that of the original sample, and the difference between the two increased with increasing temperature. This is because after the addition of S, more of the K was sulfated and fixed in the ash sample. Since the compounds such as KCl in the original sample were more easily released at high temperatures, the effect of the K being fixed in the ash due to sulfation was more obvious at higher temperatures. It should be noted that when the temperature was lower than 650 °C, the release rate of K from the sample with S/K = 6 was lower than that of the original sample. This special phenomenon may have been caused by the fact that the K-containing compounds were not released in large quantities at low temperatures, but the addition of S promoted the combustion of the sample, which increased the release of K.

The solid retention of the different occurrence forms of K in the ash for the co-combustion of CS/DL after the addition of S is shown in Figure 5. Figure 5a shows the change in the occurrence form of the K in the ash under different S/K molar ratios. As the S/K ratio increased, the content of water-soluble K in the ash continuously increased, while the contents of HCl-soluble K and insoluble K decreased. This indicates that the addition of S resulted in the sulfation of the K, so the content of water-soluble K in the ash increased, and certain quantities of the HCl-soluble K and insoluble K were converted into water-soluble K. On the basis of Figure 4a, when S/K > 6, the addition of S increased the release rate of K. In contrast, in Figure 5a, when S/K > 6, the increase in the content of the water-soluble K was no longer obvious, but the contents of HCl-soluble K and insoluble K still decreased, indicating that the K fixation effect of S had become saturated. It is generally believed that when coal and biomass are cocombusted, the S in the coal will generate a large amount of SO_2, which will be trapped by the solid phase[33] and will mainly react with inorganic alkali metal salts in the sample space to form alkali metal sulfate. The sulfur will compete with the silicates and aluminosilicates for the alkali metals.[34] A low temperature and sufficiently high sulfur content can support the formation of alkali metal sulfates.[35] In addition, it was found that as the S/K ratio increased, the contents of the NH_4Ac-soluble K and water-soluble K gradually increased. This occurred because the water-soluble K will react with the

https://doi.org/10.1021/acsomega.2c00994
ACS Omega 2022, 7, 15880−15891

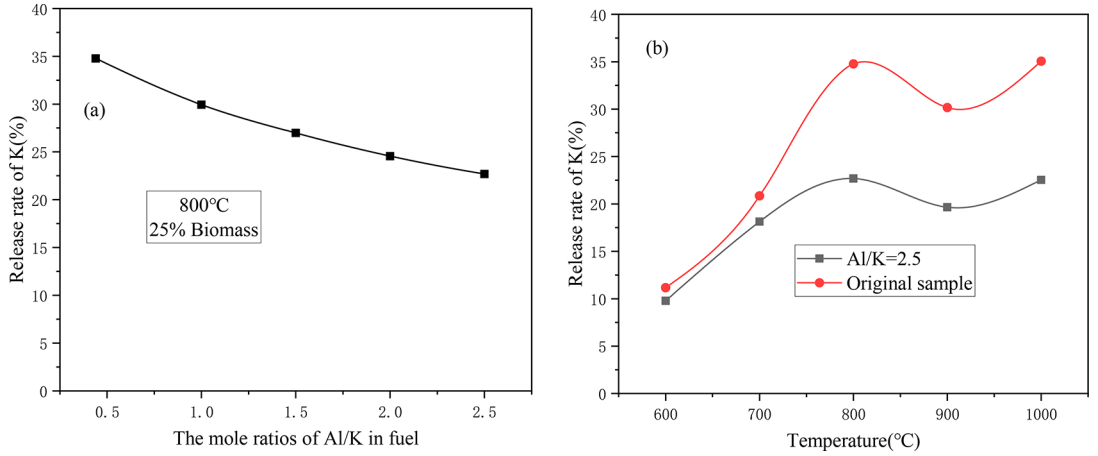

Figure 6. Effect of adding Al_2O_3 on the release rate of K for CS/DL: (a) K release rates for different Al/K molar ratios; and (b) K release rates at different temperatures.

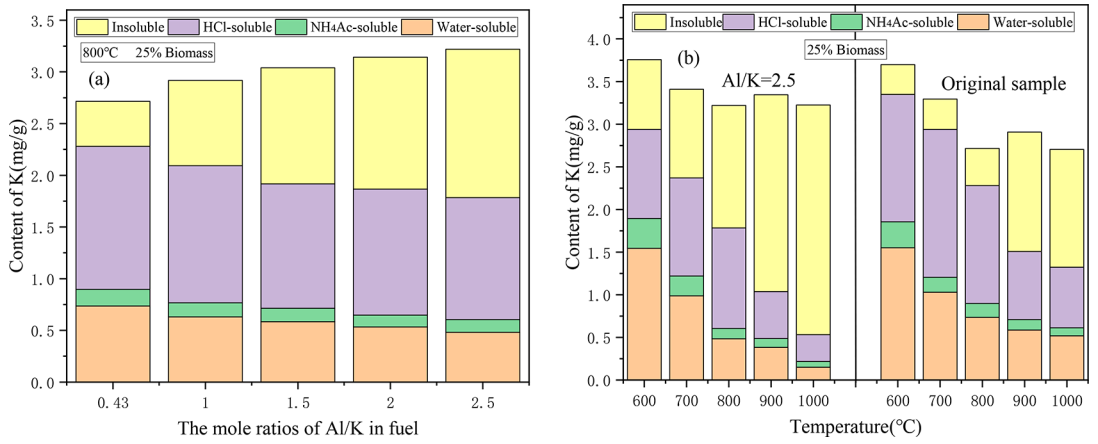

Figure 7. Effect of adding Al_2O_3 on the retentions of the different occurrence forms of K in the CS/DL ash: (a) the occurrence forms of K under different Al/K mole ratios; and (b) the occurrence forms of K at different temperatures.

SiO_2 in the ash to promote the formation of NH_4Ac-soluble K.[36]

Figure 5b shows the different occurrence forms of K in the ash of the sample with S/K = 6 and the original sample at different temperatures. After the addition of S, the content of the water-soluble K in the ash increased at all of the tested temperatures. In addition, as the temperature increased, compared with the original sample, the increase in the content of the water-soluble K in the ash was greater for the sample with S/K = 6. The reason for this phenomenon is that the increase in S led to an increase in the SO_2 concentration, which promoted the occurrence of Reaction (R1) and sulfated part of the KCl since the melting point of K_2SO_4 is higher than that of KCl. At low temperatures, less KCl was released, and the effect of sulfation on the release of K was not obvious. At high temperatures, more K_2SO_4 was produced in the combustion of the sample with S/K = 6, so more water-soluble K was fixed in the ash. In addition, the contents of the HCl-soluble K and insoluble K of the ash from sample with S/K = 6 were lower than those of the ash from the original sample at all of the tested temperatures, and the difference was more obvious at lower temperatures.

Figure 6 shows the change in the K release rate of sample CS/DL after the addition of Al_2O_3. Figure 6a shows the change in the K release rate under different Al/K molar ratios. As the Al/K ratio increased, the release rate of K gradually decreased, and the rate of decreases became smaller and smaller, which indicates that the addition of Al_2O_3 had an inhibitory effect on the release of K. According to Figure 3a, when Al/K > 1, the difference between the actual and the theoretical ash yields remained almost unchanged, which indicates that the addition of Al_2O_3 caused the K to become fixed in the ash and also promoted the release of other gaseous substances.

Figure 6b shows the K release rates of the sample with Al/K = 2.5 and the original sample under different combustion temperatures. When the temperature was between 600 and 700 °C, the difference in the release rate of K between the sample with Al/K = 2.5 and the original sample was small, signifying that the K retention capacity with the addition of Al_2O_3 was limited within this temperature range. When the temperature was higher than 700 °C, the difference between the two increased gradually, and this shows that the K retention capacity of Al_2O_3 increased gradually. When the temperature was higher than 800 °C, the difference remained almost the same, which indicates that the K retention capacity of Al_2O_3 tended to be saturated when the temperature was higher than 800 °C.

Figure 7 shows the retentions of the different occurrence forms of K in the CS/DL ash after the addition of Al_2O_3. It can be seen from Figure 7a that as the Al/K molar ratio increased,

https://doi.org/10.1021/acsomega.2c00994
ACS Omega 2022, 7, 15880−15891

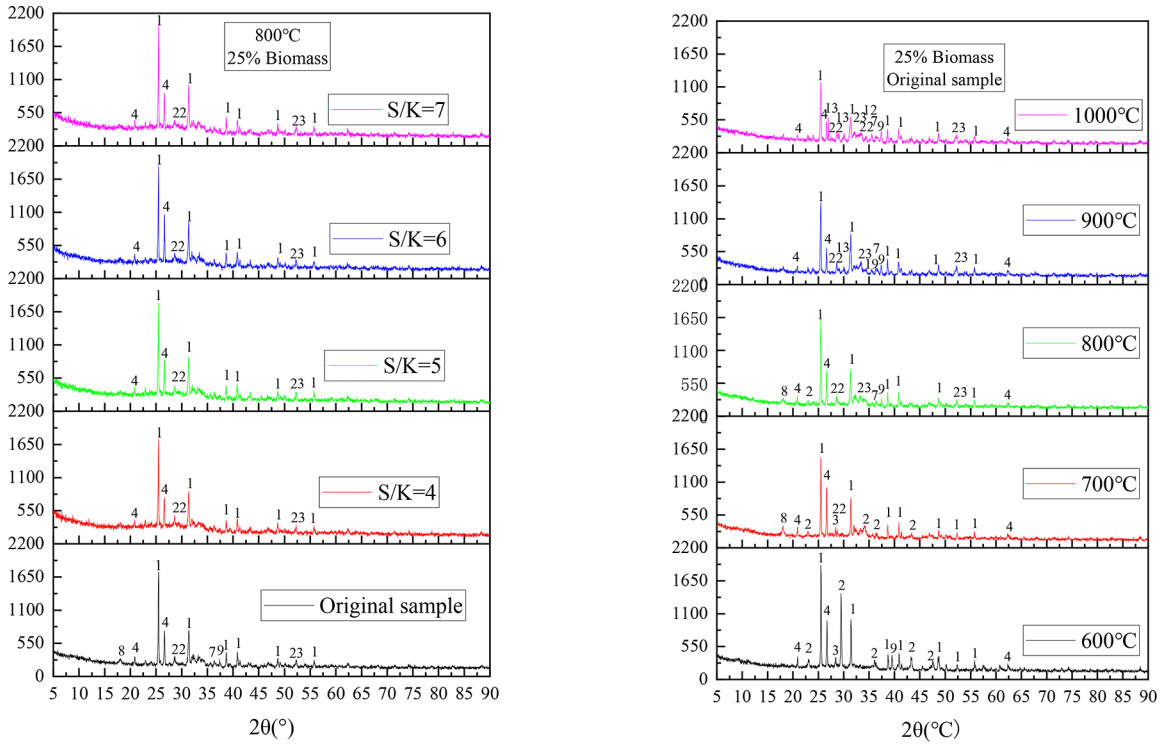

(a) XRD spectra for different S/K molar ratios (b) XRD spectra of original sample at different temperatures

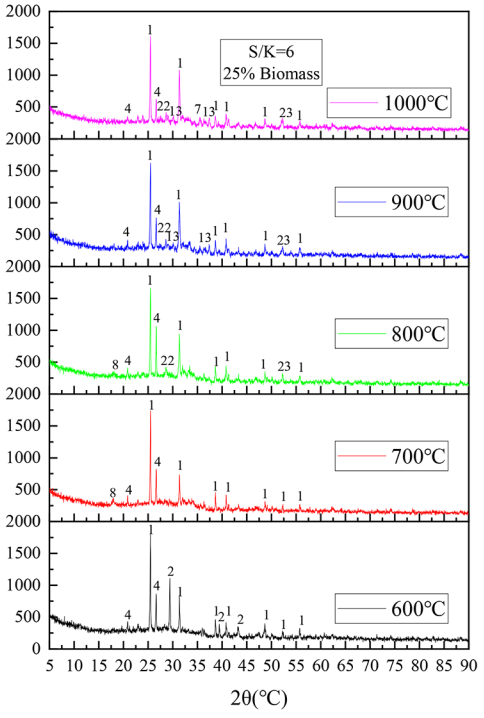

(c) XRD spectra of samples with S/K=6 at different temperatures

Figure 8. (a−c) XRD spectra of CS/XL ash after the addition of S.

the contents of both the water-soluble K and HCl-soluble K decreased, while the content of insoluble K increased significantly, which demonstrates that the addition of Al_2O_3 not only converted the water-soluble K into insoluble K, but also partially converted the HCl-soluble K into insoluble K, leaving more K in the ash.

Figure 7b shows the different forms of K in the ash of the CS/DL sample with Al/K = 2.5 and the ash of the original sample at different temperatures. When the temperature was between 600 and 700 °C, the contents of the water-soluble K in the ash of the sample with Al/K = 2.5 and the original sample were not significantly different, while the content of HCl-soluble K in the ash of the sample with Al/K = 2.5

https://doi.org/10.1021/acsomega.2c00994
ACS Omega 2022, 7, 15880−15891

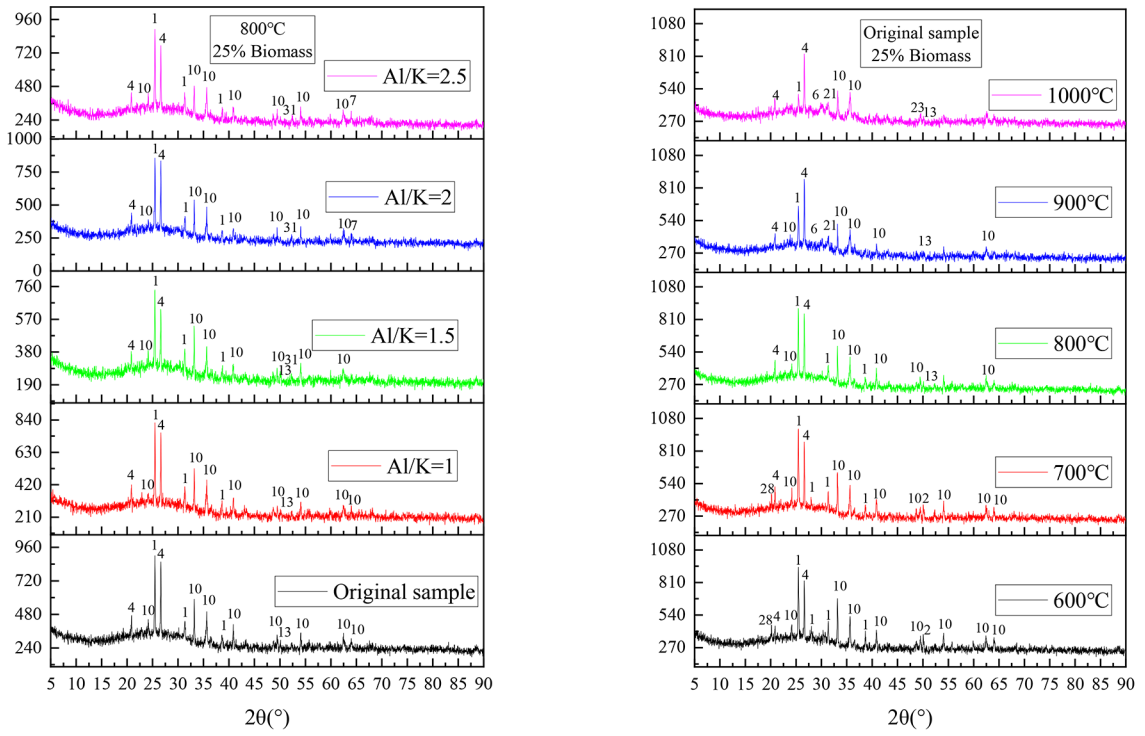

(a) XRD spectra for different Al/K molar ratios (b) XRD spectra of original sample at different temperatures

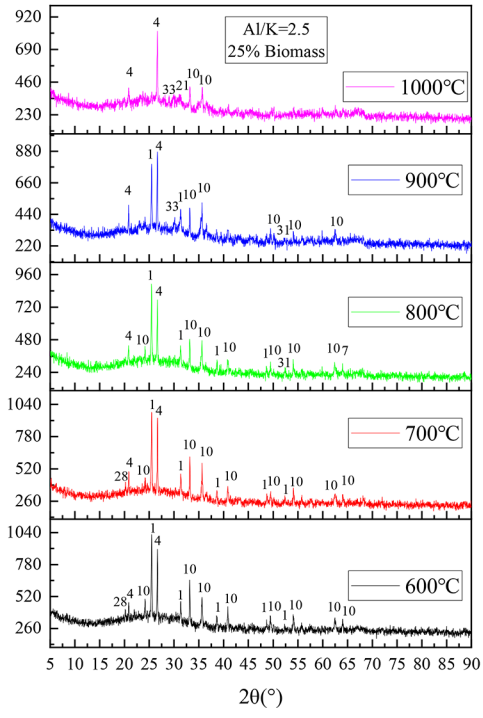

Figure 9. (a–c) XRD spectra of CS/DL ash samples after the addition of Al_2O_3.

decreased, while the content of insoluble K increased. Therefore, when the temperature was within the range of 600–700 °C, the Al_2O_3 was mainly used to convert some of the HCl-soluble K into insoluble K. When the temperature was higher than 800 °C, for the ash sample with Al/K = 2.5, the content of water-soluble K was significantly lower than that of the original sample, the content of HCl-soluble K was lower than that of the original sample, and the insoluble K content was significantly higher than that of the original sample. Therefore, when the temperature was higher than 800 °C, the addition of Al_2O_3 resulted in the conversion of the water-soluble K and HCl-soluble K into insoluble K during the combustion process. In addition to retaining more K in the ash, it also improved the ash fusion.

3.3. Effects of S and Al in Coal on Crystal Phase of Ash after Co-Combustion. Figure 8 shows the XRD spectra of the CS/XL ash samples after the addition of S. Figure 8a shows the crystalline phase of the ash samples after

https://doi.org/10.1021/acsomega.2c00994
ACS Omega 2022, 7, 15880–15891

combustion for different S/K mole ratios. There is no new K_2SO_4 peak in the ash samples after the addition of S, which is mainly due to the low K content of the raw material and the difficulty of detecting K_2SO_4 compared with KCl. However, as the addition of S increased, the $CaSO_4$ peak at $2\theta = 25.14°$ gradually strengthened, while the CaO peak at $2\theta = 37.4°$ disappeared. In addition, the $KAlSi_3O_8$ peak at $2\theta = 36.3°$ disappeared, which also corresponds to the decrease in the content of insoluble K in the ash with increasing addition of S (Figure 5a).

Figure 8b shows the XRD spectra of the ash of the CS/DL samples at different temperatures. The K in the ash sample was mainly in the form of KCl and potassium aluminosilicates. As the temperature increased, the intensity of the KCl peak gradually decreased, while the intensity of the potassium aluminosilicate peak gradually increased. In addition, as the temperature increased, the $CaSO_4$ and SiO_2 peaks decreased, and new peaks of various silicates appeared. This shows that the increase in temperature also promoted the decomposition of $CaSO_4$ and promoted the reaction between Ca and SiO_2. When the temperature was 900 °C, there was an Fe_3O_4 peak at $2\theta = 35.5°$, and when the temperature was increased to 1000 °C, this peak disappeared and an $MgFe_2O_4$ peak appeared. Thus, it is speculated that Reaction (R3) may have occurred.

$$2SO_2 + 2CaO + O_2 \rightarrow 2CaSO_4 \quad (R2)$$

$$4Fe_3O_4 + O_2(g) + 6MgO \rightarrow 6MgFe_2O_4 \quad (R3)$$

Figure 8c shows the XRD spectra of ash samples with S/K = 6 at different combustion temperatures. By comparing these spectra with that of the original sample, it was found that the spectra of the two samples combusted at 600 °C still contained a large number of $CaCO_3$ peaks, but the peak intensity of $CaCO_3$ weakened with the addition of S. The spectrum of the original sample combusted at 700 °C still contained a small number of $CaCO_3$ peaks, but $CaCO_3$ no peaks were observed after the addition of S. This indicates that the addition of S inhibited the formation of $CaCO_3$ and resulted in more Ca combining with the S to form $CaSO_4$. In addition, when the original sample was combusted at 600−700 °C, there was a KCl peak at $2\theta = 28.7°$, but it disappeared when S was added, suggesting that the addition of S promoted Reaction (R1) and caused the KCl to be sulfated into K_2SO_4. When the temperature was higher than 800 °C, the number of Ca_2SiO_4 and $KAlSi_3O_8$ peaks in the spectrum of the ash sample decreased after the addition of S, which indicates that at high temperatures, the S competed with the silicates and aluminosilicates for K and Ca.

Figure 9 shows the XRD spectra of the CS/DL sample after the addition of Al_2O_3. It can be seen from Figure 9a, when Al/K = 1.5, a new $Al_2O_3{\cdot}3CaO{\cdot}SiO_2$ peak appeared at $2\theta = 52.3°$. This may be because the addition of Al_2O_3 promoted Reaction (R4). In addition, when Al/K ≥ 2, a new $KAlSi_3O_8$ peak appears at $2\theta = 64.1°$, which may be because the addition of Al_2O_3 promoted Reactions (R5) and (R6).[32] Therefore, increasing the Al content of the mixed fuel will generally promote the formation of more aluminosilicates and will increase the content of insoluble K in the ash.

$$Al_2O_3 + 3CaO + SiO_2 \rightarrow Al_2O_3{\cdot}3CaO{\cdot}SiO_2 \quad (R4)$$

$$2KCl + Al_2O_3 + 2SiO_2 + H_2O(g) \rightarrow 2KAlSiO_4 + 2HCl(g) \quad (R5)$$

$$KAlSiO_4 + 2SiO_2 \rightarrow KAlSi_3O_8 \quad (R6)$$

The XRD spectra of the CS/DL ash samples obtained at different temperatures are shown in Figure 9b. Fe_2O_3 was common in the ash samples for all of the tested temperatures because the Fe content of DL was higher (Table 2). The Fe in the coal mainly existed in the form of FeS_2, so Reaction (R7) occurred during the combustion process. Because there was less Ca in DL than XL, a small $CaCO_3$ peak only appeared at $2\theta = 50.1°$ when 600 °C. When the combustion temperature was increased to 800 °C, a large amount of $CaCO_3$ decomposed, $CaSiO_3$ began to form, and a large amount of Al_2O_3 disappeared and began to transform into aluminosilicates. As the temperature increased to 900 and 1000 °C, two new peaks ($K_2Fe_2O_4$ and $K_6Fe_2O_5$) appeared at $2\theta = 30.1°$ and 31.4°. Because of the high content of Fe_2O_3 in the ash, it can be inferred that Reactions (R8−R10) occurred at 900 and 1000 °C.[36,37]

$$4FeS_2 + 11O_2(g) \rightarrow 2Fe_2O_3 + 8SO_2(g) \quad (R7)$$

$$Fe_2O_3 + K_2O \rightarrow K_2Fe_2O_4 \quad (R8)$$

$$Fe_2O_3 + K_2CO_3 \rightarrow K_2Fe_2O_4 + CO_2 \quad (R9)$$

$$2FeS_2 + 5O_{2(g)} + 3K_2O = K_6FeO_5 + 4SO_{2(g)} \quad (R10)$$

Figure 9c shows the XRD spectra of the ash samples with Al/K = 2.5 formed at different combustion temperatures. Through comparison with the spectra of the original samples, it was found that they exhibited several common features. As the temperature increased, the intensities of the $CaSO_4$ and Fe_2O_3 peaks gradually decreased, and a new F_6FeO_5 peak appeared at 1000 °C, which indicates that when the Al content was high, Reaction (R10) was still promoted at high temperatures. Although the intensity of the $CaSO_4$ peak decreased, calcium containing silicates such as $CaSiO_3$ and Ca_2SiO_4 appeared in the original sample. However, when Al/K = 2.5, these peaks were not observed, indicating that the addition of Al may transform these silicates into aluminosilicates. When the temperature was higher than 900 °C, a new $K_2Al_2Si_2O_8$ peak appeared at $2\theta = 30°$, and the $KAlSi_3O_8$ peak at $2\theta = 64°$ disappeared. This may be because high temperatures and high Al contents promote Reaction (R11).

$$2KAlSi_3O_8 + 2K_2O + 2Al_2O_3 \longrightarrow 3K_2Al_2Si_2O_8 \quad (R11)$$

4. CONCLUSIONS

In order to explore the influences of the S and Al in coal on the migration and transformation of K in the co-combustion of biomass and coal, elemental S and Al_2O_3 were added to blended fuel samples. The ash yield, release rate of K, occurrence forms of K, and the change in the crystal phase of the ash samples were studied under different combustion temperatures, S/K molar ratios, and Al/K molar ratios.

The S in coal is not completely released in the form of SO_2, and it is partially retained in the ash. When S/K < 6, the release rate of K decreases with increasing S content. When S/K > 6, sulfation becomes saturated, and the addition of S will promote the release of K. The release rate of K for the sample with S/K = 6 was always lower than that of the original sample at 650−1000 °C, and the higher the temperature was, the greater the difference was. As the addition of S increased, the $CaSO_4$ content increased, the content of water-soluble K compounds such as K_2SO_4 increased, and the content of insoluble K

https://doi.org/10.1021/acsomega.2c00994
ACS Omega 2022, 7, 15880−15891

compounds such as $KAlSi_3O_8$ decreased. Therefore, the S/K ratio of biomass and coal co-combustion fuel should be less than or equal to 6 in order to control the release of K and reduce the emission of SO_2.

As the Al/K ratio increased, more water-soluble K was converted into insoluble K, and the release rate of K decreased. In addition, the HCl-soluble K was converted into insoluble K. When the sample with Al/K = 2.5 and the original sample were combusted at 600−700 °C, the difference in the K release rates was relatively small. When the temperature was higher than 700 °C, the higher the temperature was, and the greater the difference in the K release rates was. This is because at high temperatures, the increase in the Al/K ratio promoted the formation of aluminosilicates containing K. Therefore, when the K content of the biomass is very high and the K release rate is also very high, the co-combustion of coal with a high Al content should be considered.

AUTHOR INFORMATION

Corresponding Author

Qian Liu − *Key Laboratory of Energy Thermal Conversion and Control of Ministry of Education, School of Energy and Environment, Southeast University, Nanjing 210096, China;* orcid.org/0000-0002-0415-4408; Email: liuqian@seu.edu.cn

Authors

Wenqi Zhong − *Key Laboratory of Energy Thermal Conversion and Control of Ministry of Education, School of Energy and Environment, Southeast University, Nanjing 210096, China*

Jun Zhou − *Key Laboratory of Energy Thermal Conversion and Control of Ministry of Education, School of Energy and Environment, Southeast University, Nanjing 210096, China*

Zuowei Yu − *Key Laboratory of Energy Thermal Conversion and Control of Ministry of Education, School of Energy and Environment, Southeast University, Nanjing 210096, China*

Complete contact information is available at: https://pubs.acs.org/10.1021/acsomega.2c00994

Author Contributions

Q.L. conceptualization, writing of the original draft. W.Z.: funding acquisition. J.Z. and Z.Y. experiments and writing. All authors have given approval to the final version of the manuscript.

Notes

The authors declare no competing financial interest.

ACKNOWLEDGMENTS

This research was supported by the National Natural Science Foundations of China [Grant No. 51976035] and the Open Foundation of the Key Laboratory for Thermal Science and Power Engineering of the Ministry of Education, Tsinghua University, China.

REFERENCES

(1) Sami, M.; Annamalai, K.; Wooldridge, M. Co-firing of coal and biomass fuel blends. *Prog. Energy Combust.* **2001**, *27* (2), 171−214.

(2) Baxter, L. Biomass-coal co-combustion: opportunity for affordable renewable energy. *Fuel* **2005**, *84* (10), 1295−1302.

(3) Spliethoff, H.; Hein, K. R. G. Effect of co-combustion of biomass on emissions in pulverized fuel furnaces. *Fuel Process. Technol.* **1998**, *54* (1), 189−205.

(4) Leckner, B. Co-combustion - A summary of technology. *Therm. Sci.* **2007**, *11* (4), 5−40.

(5) Sahu, S. G.; Chakraborty, N.; Sarkar, P. Coal-biomass co-combustion: An overview. *Renew. Sust. Energy Rev.* **2014**, *39*, 575−586.

(6) Niu, Y.; Tan, H.; Hui, S. Ash-related issues during biomass combustion: Alkali-induced slagging, silicate melt-induced slagging (ash fusion), agglomeration, corrosion, ash utilization, and related countermeasures. *Prog. Energy Combust.* **2016**, *52*, 1−61.

(7) Lupianez, C.; Mayoral, M. C.; Guedea, I.; Espatolero, S.; Diez, L. I.; Laguarta, S.; Andres, J. M. Effect of co-firing on emissions and deposition during fluidized bed oxy-combustion. *Fuel* **2016**, *184*, 261−268.

(8) Pronobis, M. Evaluation of the influence of biomass co-combustion on boiler furnace slagging by means of fusibility correlations. *Biomass Bioenergy* **2005**, *28* (4), 375−383.

(9) Mlonka-Medrala, A.; Magdziarz, A.; Kalemba-Rec, I.; Nowak, W. The influence of potassium-rich biomass ashes on steel corrosion above 550 degrees C. *Energy Convers. Manage.* **2019**, *187*, 15−28.

(10) Gogebakan, Z.; Gogebakan, Y.; Selcuk, N.; Selcuk, E. Investigation of ash deposition in a pilot-scale fluidized bed combustor co-firing biomass with lignite. *Bioresour. Technol.* **2009**, *100* (2), 1033−1036.

(11) Chen, X.; Tang, J.; Tian, X.; Wang, L. Influence of biomass addition on Jincheng coal ash fusion temperatures. *Fuel* **2015**, *160*, 614−620.

(12) Xing, P.; Darvell, L. I.; Jones, J. M.; Ma, L.; Pourkashanian, M.; Williams, A. Experimental and theoretical methods for evaluating ash properties of pine and El Cerrejon coal used in co-firing. *Fuel* **2016**, *183*, 39−54.

(13) Zhang, J.; Han, C.-L.; Yan, Z.; Liu, K.; Xu, Y.; Sheng, C.-D.; Pan, W.-P. The varying characterization of alkali metals (Na, K) from coal during the initial stage of coal combustion. *Energy Fuel* **2001**, *15* (4), 786−793.

(14) Andrea Jordan, C.; Akay, G. Speciation and distribution of alkali, alkali earth metals and major ash forming elements during gasification of fuel cane bagasse. *Fuel* **2012**, *91* (1), 253−263.

(15) Werkelin, J.; Skrifvars, B. J.; Zevenhoven, M.; Holmbom, B.; Hupa, M. Chemical forms of ash-forming elements in woody biomass fuels. *Fuel* **2010**, *89* (2), 481−493.

(16) Zevenhoven, M.; Yrjas, P.; Skrifvars, B. J.; Hupa, M. Characterization of Ash-Forming Matter in Various Solid Fuels by Selective Leaching and Its Implications for Fluidized-Bed Combustion. *Energy Fuel* **2012**, *26* (10), 6366−6386.

(17) Wei, X.; Lopez, C.; Von Puttkamer, T.; Schnell, U.; Unterberger, S.; Hein, K. R. G. Assessment of chlorine-alkali-mineral interactions during co-combustion of coal and straw. Energ. *Fuel* **2002**, *16* (5), 1095−1108.

(18) Glazer, M. P.; Khan, N. A.; De Jong, W.; Spliethoff, H.; Schürmann, H.; Monkhouse, P. Alkali metals in circulating fluidized bed combustion of biomass and coal: Measurements and chemical equilibrium analysis. *Energy Fuel* **2005**, *19* (5), 1889−1897.

(19) Yang, T.; Kai, X.; Sun, Y.; He, Y.; Li, R. The effect of coal sulfur on the behavior of alkali metals during co-firing biomass and coal. *Fuel* **2011**, *90* (7), 2454−2460.

(20) Johansen, J. M.; Aho, M.; Paakkinen, K.; Taipale, R.; Egsgaard, H.; Jakobsen, J. G.; Frandsen, F. J.; Glarborg, P. Release of K, Cl, and S during combustion and co-combustion with wood of high-chlorine biomass in bench and pilot scale fuel beds. *P. Combust. Inst.* **2013**, *34* (2), 2363−2372.

(21) Li, R.; Kai, X.; Yang, T.; Sun, Y.; He, Y.; Shen, S. Release and transformation of alkali metals during co-combustion of coal and sulfur-rich wheat straw. *Energy Convers. Manage.* **2014**, *83*, 197−202.

(22) Theis, M.; Skrifvars, B. J.; Zevenhoven, M.; Hupa, M.; Tran, H. Fouling tendency of ash resulting from burning mixtures of biofuels. Part 2: Deposit chemistry. *Fuel* **2006**, *85* (14−15), 1992−2001.

(23) Wang, L.; Skreiberg, O.; Becidan, M.; Li, H. Investigation of rye straw ash sintering characteristics and the effect of additives. *Appl. Energy* **2016**, *162*, 1195−1204.

(24) Shen, Y.; Hu, Y.; Wang, M.; Bao, W.; Chang, L.; Xie, K. Speciation and thermal transformation of sulfur forms in high-sulfur coal and its utilization in coal-blending coking process: A review. *Chin. J. Chem. Eng.* **2021**, *35*, 70−82.
(25) Tian, L.; Yang, W.; Chen, Z.; Wang, X.; Yang, H.; Chen, H. Sulfur behavior during coal combustion in oxy-fuel circulating fluidized bed condition by using TG-FTIR. *J. Energy Inst.* **2016**, *89*, 264−270.
(26) De, S.; Assadi, M. Impact of cofiring biomass with coal in power plants − A techno-economic assessment. *Biomass Bioenergy* **2009**, *33* (2), 283−293.
(27) Liu, Y.; Cheng, L.; Zhao, Y.; Ji, J.; Wang, Q.; Luo, Z.; Bai, Y. Transformation behavior of alkali metals in high-alkali coals. *Fuel. Process Technol.* **2018**, *169*, 288−294.
(28) Aho, M.; Ferrer, E. Importance of coal ash composition in protecting the boiler against chlorine deposition during combustion of chlorine-rich biomass. *Fuel* **2005**, *84* (2), 201−212.
(29) Arvelakis, S.; Jensen, P. A.; Dam-Johansen, M. Simultaneous thermal analysis (STA) on ash from high-alkali biomass. *Energy Fuel* **2004**, *18* (4), 1066−1076.
(30) Mason, P. E.; Darvell, L. I.; Jones, J. M.; Williams, A. Observations on the release of gas-phase potassium during the combustion of single particles of biomass. *Fuel* **2016**, *182*, 110−117.
(31) Yang, Y. B.; Sharifi, V. N.; Swithenbank, J.; Ma, L.; Darvell, L. I.; Jones, J. M.; Pourkashanian, M.; Williams, A. Combustion of a Single Particle of Biomass. *Energy Fuel* **2008**, *22* (1), 306−316.
(32) Xue, Z.; Zhong, Z.; Zhang, B.; Zhang, J.; Xie, X. Potassium transfer characteristics during co-combustion of rice straw and coal. *Appl. Therm. Eng.* **2017**, *124*, 1418−1424.
(33) Davidsson, K. O.; Amand, L. E.; Leckner, B.; Kovacevik, B.; Svane, M.; Hagstrom, M.; Pettersson, J. B. C.; Pettersson, J.; Asteman, H.; Svensson, J. E.; Johansson, L. G. Potassium, chlorine, and sulfur in ash, particles, deposits, and corrosion during wood combustion in a circulating fluidized-bed boiler. *Energy Fuel* **2007**, *21* (1), 71−81.
(34) Shah, K. V.; Cieplik, M. K.; Betrand, C. I.; van de Kamp, W. L.; Vuthaluru, H. B. Correlating the effects of ash elements and their association in the fuel matrix with the ash release during pulverized fuel combustion. *Fuel Process. Technol.* **2010**, *91* (5), 531−545.
(35) Schuermann, H.; Monkhouse, P. B.; Unterberger, S.; Hein, K. R. G. In situ parametric study of alkali release in pulverized coal combustion: Effects of operating conditions and gas composition. *P. Combust. Inst.* **2007**, *31* (2), 1913−1920.
(36) Lin, W. G.; Dam-Johansen, K.; Frandsen, F. Agglomeration in bio-fuel fired fluidized bed combustors. *Chem. Eng. J.* **2003**, *96* (1−3), 171−185.
(37) Chi, H.; Pans, M. A.; Sun, C.; Liu, H. An investigation of lime addition to fuel as a countermeasure to bed agglomeration for the combustion of non-woody biomass fuels in a 20kWth bubbling fluidised bed combustor. *Fuel* **2019**, *240*, 349−361.

https://doi.org/10.1021/acsomega.2c00994
ACS Omega 2022, 7, 15880−15891